Received: 2 May 2023 | Revised: 14 July 2023 | Accepted: 27 July 2023

DOI: 10.1002/biot.202300194

Biotechnology Journal

RESEARCH ARTICLE

Impact of ethanol on continuous inline diafiltration of liposomal drug products

Robert D. Worsham[1,2] | **Vaughan Thomas**[2] | **Suzanne S. Farid**[2]

[1]Insmed, Inc., Bridgewater, New Jersey, USA

[2]Department of Biochemical Engineering, University College London, London, UK

Correspondence
Robert D. Worsham, Insmed, Inc., Bridgewater, NJ, USA.
Email: robert.worsham@insmed.com

Abstract

Liposomal drug products are playing an increasing role in the field of drug delivery. With this increased demand comes the need to increase the capabilities and capacity of manufacturing options. Continuous manufacturing techniques present a significant opportunity to address these needs for liposomal manufacturing processes. Liposomal formulations have unique considerations that impact translation from batch to continuous process designs. This article examines aspects of converting to a continuous design that were previously viewed as inconsequential in a batch process. The batch process involves the removal of ethanol (EtOH) through tangential flow filtration (TFF). EtOH was found to reduce the permeability of the hollow fibers used for TFF. This effect was determined to have minimal impact on the overall batch process design but considerable influence on the design of continuous TFF such as inline diafiltration (ILDF). Using a pilot scale setup, EtOH was found to decrease permeability in an inverse manner to EtOH concentration. Further assessment found that dilution of the EtOH levels prior to diafiltration can significantly reduce the amount of ILDF stages needed and that a continuous design requires less buffer to the commensurate batch design.

KEYWORDS
continuous manufacturing, inline diafiltration (ILDF), liposomes, single-use, tangential flow filtration (TFF)

1 | INTRODUCTION

Liposomes are nano-scale spherical-shaped vesicles comprised of one or more phospholipid bilayers, that have the ability to encapsulate hydrophilic or lipophilic drugs for the purposes of targeted drug delivery.[1] A number of strategies have been demonstrated for liposome manufacture but have suffered from the lack of reliable methods with sufficient throughput to enable a commercial scale.[2–4] Strategies for liposome synthesis focus on addressing and optimizing one or several of the key driving forces of vesicle assembly including the component solubilities, concentrations, and process thermodynamic parameters (i.e., temperature, pressure, etc.).[2,3] Manufacturing methods can be designed to fine-tune liposomes with various properties and, in doing so, can lend both advantages and disadvantages amenable to large-scale processing. In addition, selection of the manufacturing method often depends on the end product requirements for clinical efficacy including liposome size and size distribution, lipid composition, and the drug release characteristics, which together dictate the pharmacokinetic demonstration of adsorption, distribution, metabolism, and elimination (ADME).

Abbreviations: ADME, adsorption, distribution, metabolism, and elimination; API, active pharmaceutical ingredient; ATF, alternating tangential flow filtration; CVDF, constant volume diafiltration; EtOH, ethanol; HPLC, high-performance liquid chromatography; ILDF, inline diafiltration; TFF, tangential flow filtration.

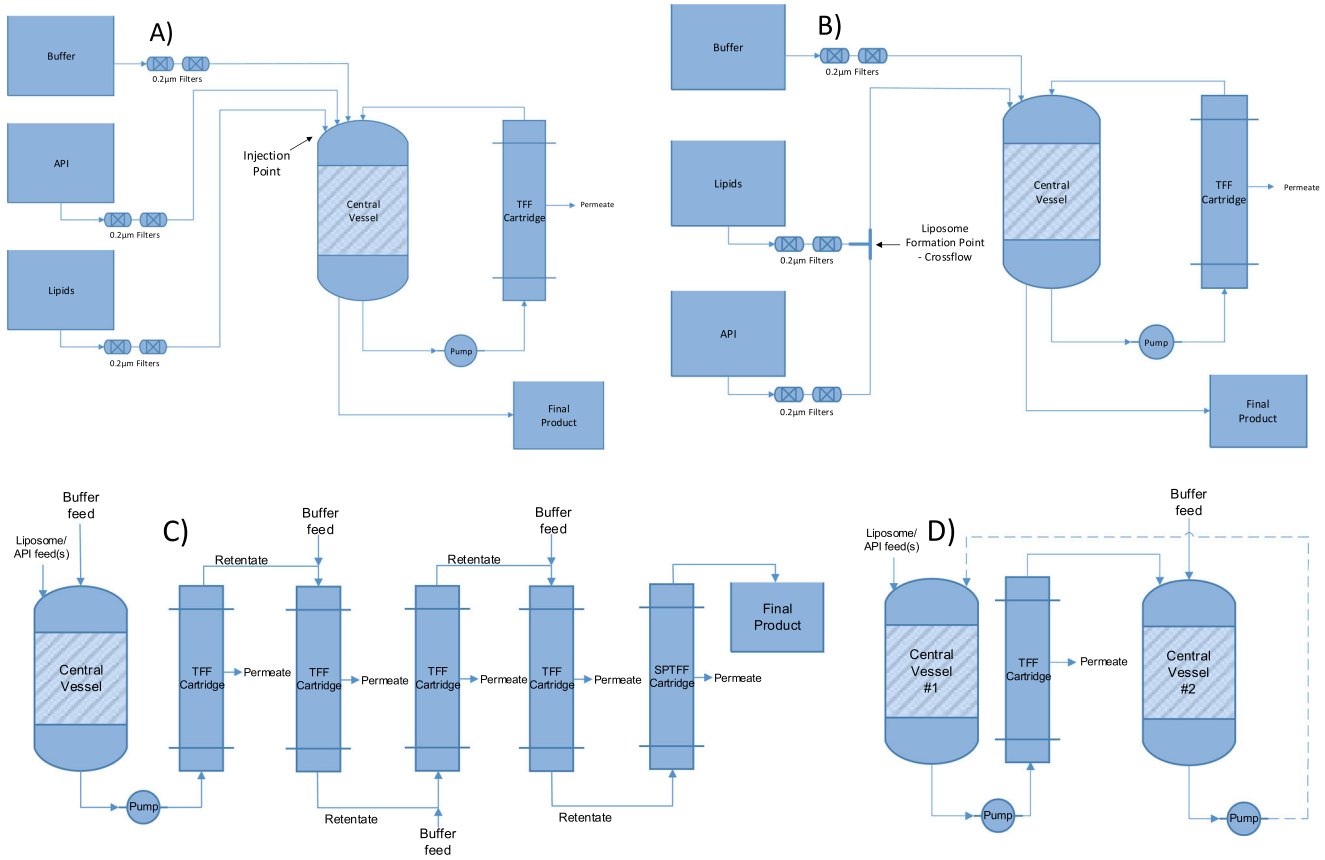

FIGURE 1 Liposomal drug product manufacturing process flow diagrams. (A) Batch design, ethanol/ether injection method: lipid/solvent solution is directly fed into the central vessel. Formulations are refined in multi-step buffer exchange diafiltration and concentration steps. (B) Batch design, crossflow method: solvent/anti-solvent mix in-line at an intersection point. Formulations are refined in multi-step buffer exchange diafiltration and concentration steps. (C) Inline-diafiltration (ILDF) design: proposed novel process design for continuous liposome drug product manufacturing. Multistage single-pass concentration with inline buffer exchange. Number of passes/stages required is dependent on process/product. Solution vessels and liposome formation equipment not shown. (D) Simulated ILDF set-up: process flow diagram of the single-pass concentration/buffer exchange, which can be used to simulate ILDF with the ability to analysis retentate/permeate in between passes/stages. Solution vessels and liposome formation equipment not shown. The dashed line indicates the bulk is not returned to central vessel #1 until after analysis/dilution of its entirety.

The most successful examples of scaled methods for liposome manufacture to date have followed the principles of alcohol injection (Figure 1A) or crossflow techniques (Figure 1B), wherein dissolved lipids are precipitated from an organic solvent into an aqueous solution (anti-solvent) by means of reciprocal diffusion of the organic and aqueous phases.[5,6–9] A change in the local solubility of the lipids during this process ultimately leads to the spontaneous formation of liposomes that encapsulate a small volume of the aqueous solution. Depending on the chemical nature of the active pharmaceutical ingredient (API), it can be encapsulated in the aqueous core or embedded in the lipid layer. The critical parameters for the formation of liposomes by this method are residence time and geometry of the mixing/intersection of organic-solvated lipid and the antisolvent which are dictated by programmed flow conditions. After liposome formation, the mixture containing undesired organic solvent and unencapsulated API can then be refined to the desired formulation strength and composition using tangential flow filtration (TFF) or similar methods.[7,10,11]

The aforementioned production methods were designed to operate as a batch process, but the crossflow method is based on a liposome formation step which is continuous in its inherent mechanism (Figure 1B). So long as each feed stream is continuously fed, liposomes will be continuously generated. With continuous formulation of the feed solutions, the liposome formation step can proceed indefinitely. By implementing a continuous version of TFF, which supports refinement of the drug product to the desired end formulation, continuous manufacturing of liposomal drug products is a feasible concept.

Continuous versions of TFF have been explored for similar applications in the biologics sector. For continuous perfusion cell culture, the industry has moved from internal spin-filters to external retention devices such as alternating tangential flow filtration (ATF) or TFF systems for media exchange.[12–14] Single pass tangential flow filtration (SPTFF) has been evaluated for cell culture harvest concentration and for protein concentration allowing this process step to happen in a continuous fashion instead of the batch mode required by traditional TFF.[15–20] TFF concentrates product through multiple passes of a recirculating loop while SPTFF concentrates in an inline fashion with a single pass through multiple TFF cassettes in series. SPTFF enables product to be continuously fed to the next unit operation

or process step with the additional benefits of lower system hold-up volumes. Designs for multiple SPTFFs in series, such as the Cadence In-line Diafiltration Module (ILDF), are becoming available and have been explored.[21] Applying the ILDF design as the TFF/formulation refinement step in a continuous process is shown in Figure 1C.

Previous work with continuous TFF designs has focused on biologics manufacture. To date, no examination of continuous TFF designs have been performed for liposomal drug product manufacture. This paper investigates the impact of the organic solvent used in liposome formation, namely ethanol (EtOH), on the design of continuous inline diafiltration for a liposomal drug product. To explore the continuous TFF/formulation refinement for liposomal drug product, a pilot scale ILDF system mimicking Figure 1C was explored (Figure 1D). The set up in Figure 1D evaluated a simulated ILDF configuration by analyzing each concentration pass and dilution step individually with the objective of determining the number of passes/stages and the buffer consumption needed to achieve target solvent removal. The results were compared to the batch process option.

2 | METHODS

2.1 | Feed materials

The API used is this formulation is amikacin. Amikacin is an aminoglycoside used as an antibiotic in the treatment of various bacterial infections. The amikacin solution was prepared by dissolving amikacin sulfate (CAS 39831-55-5) in water-for-injections (WFI) or deionized water at 45 mg mL^{-1} amikacin base and pH adjusted to 6.7 using NaOH.

The lipid solution was prepared by dissolving Dipalmitoylphosphatidylcholine (DPPC) and cholesterol at a 2:1 weight ratio in 100% EtOH at 20 mg mL^{-1}.

The buffer solution consists of 1.5% NaCl in WFI or deionized water.

2.2 | Batch processing

The batch process for manufacturing liposomal drug product, as depicted in Figure 1B, involves mixing/infusing streams of lipid solution and amikacin solution at the crossflow point in an approximate 1:2 ratio. The magnitude of these flow rates is dependent on the scale of the process. The output of the crossflow point ("liposome mixture") is fed into a central vessel concurrently with the buffer solution. Constant volume diafiltration (CVDF) is performed using a 50 kDa Cytiva hollow fiber cartridge (UFP-500-E-85MSM) until six diavolumes have been processed. The product is then concentrated through the hollow fiber membrane until the retentate reaches 70 mg mL^{-1} amikacin base.

2.3 | Simulated ILDF system

The simulated ILDF system consists of the same or similar equipment used in the batch process. The equipment was arranged in a manner supporting multiple independent concentration/buffer exchange passes with opportunity for sampling and dilution with buffer in between each pass (Figure 1D). The hollow fiber cartridge was not replaced in between passes. A new hollow fiber was used for each bulk run on the simulated ILDF system.

The starting solutions and liposome mixture as described previously were used as a starting material. The buffer solution was used to predilute the liposome mixture as described in Section 3.

2.4 | Analytical methods

Total amikacin concentrations were measured by high-performance liquid chromatography (HPLC) using a Hypersil GOLD C18 column (175 Å, 3 μm, 150 mm × 4.6 mm) with a mobile phase of 65% methanol, 35% water, and 0.3% pentafluoropropionic acid (PFPA). An aliquot of each liposome suspension was centrifuged in an Amicon Ultra-0.5 centrifugal filter unit with Ultracel-30 kDa membrane to separate free amikacin, and the amount of unencapsulated amikacin was then determined by HPLC.

Lipid concentrations were measured by HPLC using an XBridge C8 column (130 Å, 3.5 μm, 150 mm × 4.6 mm) with a mobile phase A consisting of 49.9% acetonitrile, 49.9% water, 0.1% acetic acid, and 0.1% triethylamine and mobile phase B consisting of 44.9% acetonitrile, 45% isopropyl alcohol, 10% water, 0.1% acetic acid, and 0.1% triethylamine.

Residual EtOH or EtOH concentrations were measured by using gas chromatography (GC) using a Duraguard DB.

3 | RESULTS

In this section, the batch process diafiltration was assessed keeping in mind the desire to convert to a continuous diafiltration or ILDF configuration. These learnings were then applied to an experimental set up (Figure 1D), designed to mimic the ILDF configuration. These results were evaluated for trends and optimal conditions with respect to an ILDF process.

3.1 | Batch process

In order to properly compare batch to continuous TFF performance, the batch TFF must be better understood. The process begins with the liposome formation mixture entering the central vessel at the same time as the buffer. At the completion of the liposome formation step, the central vessel contains approximately 30% EtOH, which is slightly less than the undiluted liposome formation mixture due to the dilution from the added buffer stream.

The batch TFF operates as CVDF with constant inlet pressure to the hollow fiber. Permeate flow is fully open with no applied back pressure. The buffer stream flow matches the permeate flow to maintain constant volume.

Evaluation of the batch TFF performance showed an unexpected phenomenon. Regardless of the constant inlet pressure, the permeate

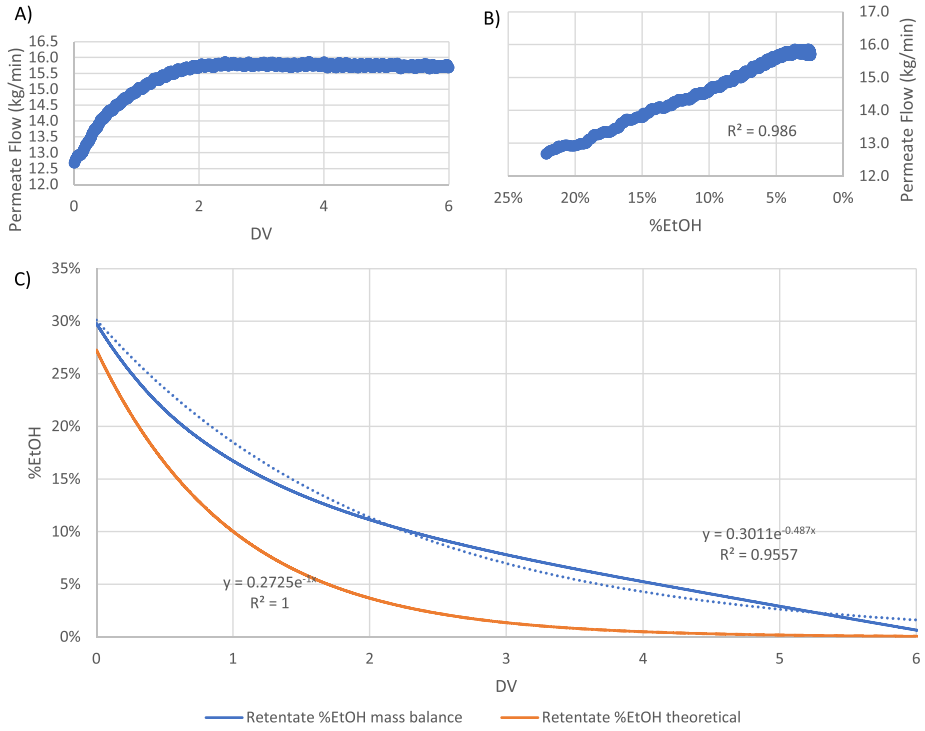

FIGURE 2 Batch process constant volume diafiltration (CVDF) data plots. (A) Permeate flow versus diavolumes: the permeate flow increases and levels off as diavolumes progress. (B) Permeate flow versus ethanol concentration: the permeate flow increases linearly as the ethanol concentration decreases. (Note the decreasing x-axis in order to maintain the left-to-right chronology of the data.) (C) Ethanol (EtOH) concentration of batch retentate versus diavolumes as compared to a theoretical diafiltration curve with $\alpha = 0$ rejection coefficient. The actual batch process rejection coefficient for EtOH calculates to approx. 0.5.

flow showed an increasing pattern as the diavolumes progressed as opposed to a constant flow. Shown in Figure 2A, permeate flow increased and leveled off through the run. Further assessment of the permeate showed that the EtOH concentration decreased linearly as the permeate flow increased (Figure 2B), indicating permeate flow and EtOH concentration may be interrelated.

EtOH would be expected to be removed during TFF in a manner following the standard diafiltration equation (Equation 1) such that c_0 = initial EtOH concentration, c = final EtOH concentration, α = EtOH rejection coefficient, and $\frac{V_b}{V_s}$ = diavolumes.

$$c = c_0 e^{-(1-\alpha)\frac{V_b}{V_s}} \quad (1)$$

It is common to assume the species being removed is free flowing and has a rejection coefficient of 0. The results in Figure 2B indicate a relationship between the EtOH concentration and the permeate flow. The EtOH most likely has an impact on hollow fiber permeability, which could be expressed as EtOH having a partial rejection coefficient (α). This is not unprecedented as EtOH has shown hollow fiber swelling and impact on permeability in other industrial applications.[22,23]

To assess the EtOH rejection coefficient, the batch process was assessed with the Equation (1) model. Using an inline density measurement on the permeate, the EtOH concentration was calculated across the diavolumes. Applying mass balance for the system, the retentate EtOH concentration was calculated, and the curve fitted to Equation (1) to determine the EtOH rejection coefficient. As shown in Figure 2C, the rejection coefficient (α) calculated to approx. 0.5 as opposed to the zero coefficient that would have been assumed. Additionally, the fit showed the rejection coefficient to be slightly greater than 0.5 early in the process and slightly less than 0.5 later in the process, indicating an EtOH concentration dependency to the rejection coefficient.

While not having a significant impact on the overall batch process, an EtOH concentration dependent rejection coefficient is interesting to consider in a continuous TFF/ILDF system. In the system shown in Figure 1C, the initial hollow fiber pass/stage of the ILDF system would contain higher concentrations of EtOH and would presumably be less efficient/permeable than the later hollow fiber passes/stages. Thus, more passes would be needed to remove the first portion of the EtOH as compared to later portions. Based on this, additional upfront dilution of the initial liposome formation mixture should increase permeability and efficiency and reduce the amount of passes/stages needed in a continuous design.

The EtOH concentration dependency phenomenon was further explored regarding its impact on the continuous ILDF arrangement under the guise that dilution/increased permeability decreases the number of passes/stages needed and increases overall efficiency/benefit of the system.

3.2 | Continuous inline diafiltration

3.2.1 | Hollow fiber passes and ethanol rejection coefficient

Continuous ILDF was explored using the arrangement shown in Figure 1D to mimic the arrangement in Figure 1C, but with the ability to analyze the output of each pass/stage. The entirety of the bulk of the liposome formation mixture was fed through the hollow fiber as a single pass into the second vessel. The retentate and permeate were analyzed, buffer added to replace the permeate, then the entirety of the adjusted bulk returned to the first vessel in preparation for another pass. This was repeated until the target EtOH removal was achieved. The intent was to simulate the arrangement in Figure 1C with the ability to assess the output of each pass/stage discretely.

The assessment of the continuous ILDF arrangement involved processing the post-liposome formation bulk mixture with various levels of pre-dilution from undiluted (36% EtOH) to significantly diluted (5% EtOH). The EtOH concentration was assessed after each pass/stage and the process repeated.

Figure 3A,B show the results of the various initial EtOH concentrations and the EtOH removal curves over the repeated passes. As expected, EtOH concentration was reduced with each pass and the number of passes needed to remove the EtOH decreased with decreased initial EtOH concentrations. For example, an initial concentration of 24% EtOH required 36 passes for target removal while starting at 5% EtOH required nine passes. The behavior of the curves followed the pattern of the diafiltration model (Equation 1) with passes in place of diavolumes, but with a notable exception. Unexpectedly, the fitted curves for the simulated ILDF results showed a variable exponent. The exponent, where the rejection coefficient is contained in the traditional diafiltration equation (Equation 1), was expected to be constant, but instead, decreased as the initial EtOH concentration decreased. This supports the previous notion of an EtOH concentration dependent rejection coefficient.

From this, a continuous ILDF equation (Equation 2) was derived where c_0 = initial EtOH concentration (%), c = final EtOH concentration (%), N_p = number of simulated ILDF passes and α = EtOH rejection coefficient. The EtOH rejection coefficient is dependent on the initial EtOH concentration, $\alpha = f(c_0)$. This function was derived from the results in Figure 3A,B as shown in Figure 3C and represented with Equation (3).

$$c = c_0 e^{-(1-\alpha)N_p} \tag{2}$$

$$\alpha = f(c_0) = 0.059 \ln(c_0) + 0.99, \{0 < c_0 < 0.4\} \tag{3}$$

3.2.2 | Simulated ILDF permeate

Before fully applying the above equations to continuous ILDF systems, aspects of the permeate stream should be considered. Figure 3D shows the amount of permeate collected with each pass for the various initial EtOH concentration runs (not all are show for visual simplicity). As initial EtOH concentration decreased, the amount of permeate collected increased. Additionally, as the EtOH concentration decreased with each pass, the amount of permeate collected increased and plateaued, but did not reach the same level as the plateaus for other initial concentration runs. For example, 24% initial EtOH concentration started at 4.5 kg per pass and plateaued at approx. 8 kg per pass, 15% initial EtOH concentration started at 7 kg per pass and plateaued at approx. 10 kg per pass, and 7.5% initial EtOH concentration started at 10.5 kg per pass and plateaued at approx. 12 kg per pass.

Figure 3E shows the permeate flow rates versus the retentate EtOH concentration for each pass for various initial EtOH concentration runs (not all are show for visual simplicity). Similar to the permeate collected in Figure 3D, flow rates increased as EtOH concentrations decreased and peak flow rates increased with decreasing initial EtOH concentration. Specifically, 24% initial EtOH concentration started at 4 kg min^{-1} permeate flow and peaks at approx. 9 kg min^{-1} while starting with 7.5% EtOH gave 10.7 kg min^{-1} and peaked with approx. 13 kg min^{-1}. It would be expected that a given EtOH concentration would yield a given flow rate, similar to the EtOH concentration/permeate flow rate results in Figure 2B (permeate flow vs. EtOH concentration). Instead, when the initial EtOH concentrations of 24%, 15%, and 7.5% were reduced to 5%, for example, the flow rates were 7.5, 9.0, and 11.3 kg min^{-1}, respectively.

This indicates that hollow fiber permeability is not only impacted and dependent on EtOH concentration during the process but is set by the initial EtOH concentration exposure and only able to recover a limited amount of performance. Stated another way, when the EtOH concentration levels between runs are equivalent in the retentate, it does not correlate to a specific permeability, but rather permeability is set by the initial EtOH concentration and will only improve a relative amount. This aligns with the other plot in Figure 2A (permeate flow rate vs. DV). Figure 2A captures the plateau effect, but not the effect of the initial EtOH concentration since there is only one initial concentration.

Once the hollow fiber was exposed to the initial concentration in the Figure 1D set up, the permeability was set and overall performance limited. Therefore, the Figure 1D set up is not a fully valid representation of a continuous ILDF process. The Figure 1D set up used the same single hollow fiber to facilitate all passes/stages for each run, whereas a continuous ILDF process like Figure 1C would have individual hollow fibers for each pass/stage. More appropriately, the permeate values for only the initial EtOH concentration passes should be used and extrapolated; these values being accurate representations of the initial EtOH exposures of some of the independent hollow fibers in a continuous ILDF set up (Figure 1C).

3.2.3 | Extrapolated ILDF stage requirements

Using the permeate removal data for the initial pass of the five starting EtOH concentrations examined, a continuous ILDF (Figure 1C) was modeled and the number of passes/stages for the target EtOH removal calculated. Figure 4A shows the permeate removed for each of

A) Starting Concentration %EtOH	No. of Passes to <1%EtOH/Target Density	Fitted Diafiltration Equation	Simulated ILDF "Rejection Coefficient" (α)	Coefficient of determination (R^2)
36%	53 (extrapolated)	$y = 0.35e^{-0.051x}$	0.949	0.995
24%	36	$y = 0.30e^{-0.088x}$	0.912	0.979
15%	24	$y = 0.17e^{-0.117x}$	0.883	0.994
7.5%	13	$y = 0.08e^{-0.166x}$	0.834	0.998
5%	9	$y = 0.05e^{-0.176x}$	0.824	0.999

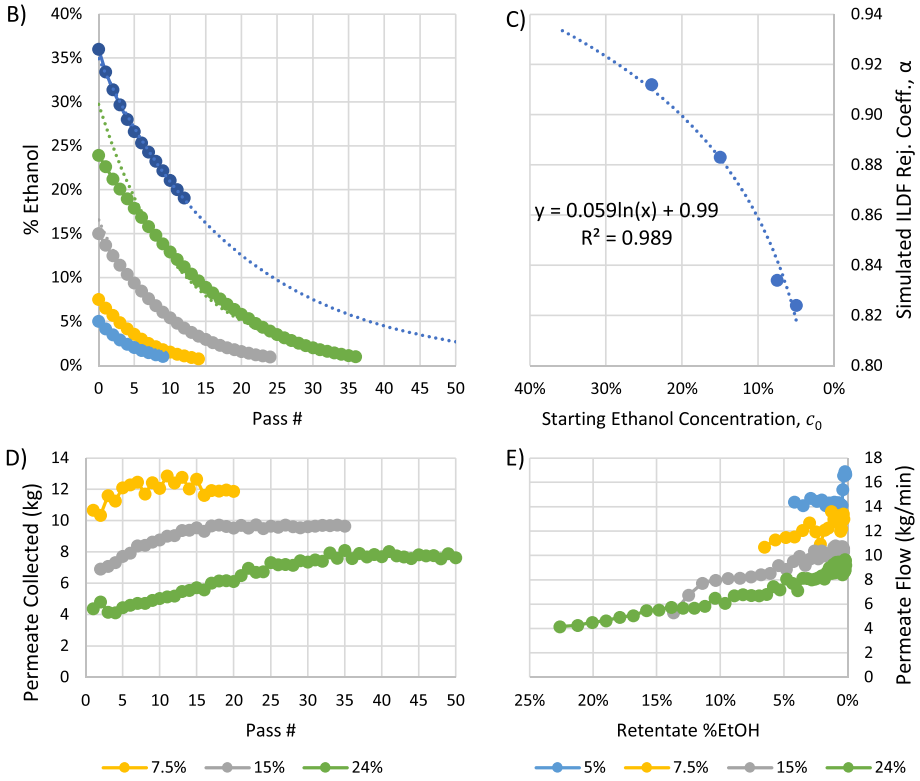

FIGURE 3 Simulated inline-diafiltration (ILDF) data plots.(A, B) Ethanol removal curves and total passes required to meet the ethanol removal target for various starting ethanol concentrations. (C) Calculated function for the ethanol concentration dependent rejection coefficient for the simulated ILDF in Figure 1D. (D) Permeate collected from each hollow fiber concentration pass for various starting ethanol concentration runs. (E) Permeate flow rate versus the retentate ethanol concentration for each hollow fiber concentration pass for various starting ethanol concentration runs. (Note: (C) and (E) have a decreasing x-axis in order to maintain the left-to-right chronology of the data.)

the measured initial EtOH concentration passes with an extrapolated curve/function. This function was used to model each independent pass/stage of a continuous ILDF process until the target EtOH removal was achieved (Figure 4B). Each pass/stage was modeled using the following equations:

$$c_{p+1} = \frac{c_p R - c_p P}{R} \quad (4)$$

$$P = -5.696 \ln(c_p) - 3.8359, \{0 < c_p < 0.4\} \quad (5)$$

where c_p = EtOH concentration at the beginning of a pass (%), c_{p+1} = EtOH concentration at the end of a pass (%), R = mass of the retentate (kg), and P = permeate mass as a function of the incoming EtOH concentration (kg). Using Equations 4 and 5, starting EtOH concentrations were selected and the EtOH concentrations calculated after each subsequent pass/stage. The calculation continued until the target EtOH removal was achieved and the number of passes/stages determined.

The number of passes needed when starting at different concentrations was calculated and are shown in Figure 4B. Figure 4C compares the calculated pass/stage data to the pass/stage data determined with the Figure 1D set up. The modeled continuous ILDF passes required are significantly less than the Figure 1D set up, but the difference becomes smaller with lower initial EtOH concentrations. This shows that the impact of carrying through the

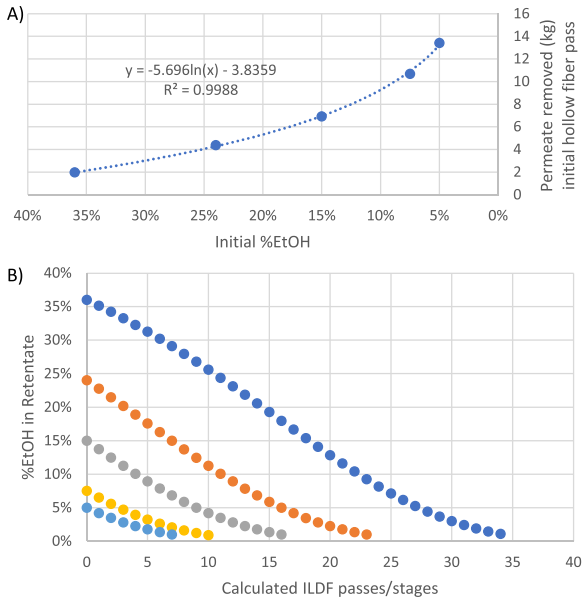

C) Initial %EtOH	Extrapolated ILDF passes/stages	ILDF passes/stages based in Figure 1D set up
36%	35	53
24%	23	36
15%	16	24
7.5%	10	13
5%	7	9

FIGURE 4 Calculated inline-diafiltration (ILDF) data based on initial ethanol concentration passes. (A) Permeate removed at initial ethanol concentration passes and the extrapolated function. (B) Calculated number of passes/stages to achieve target ethanol removal given the initial ethanol concentrations for each independent hollow fiber/pass/stage. (C) Comparison of the extrapolated and simulated amount of required ILDF passes/stages required to achieve target ethanol removal.

Figure 1D initial EtOH concentration limitation on permeability was mitigated by calculating the passes independently. Note that the continuous ILDF EtOH reduction curve does not follow the diafiltration equation, while the Figure 1D set up did. This is most likely due to the Figure 1D reuse of the same hollow fibers for each run, which caused the permeability limitations similar to a CVDF batch process. The extrapolated ILDF model's use of new hollow fibers for each pass/stage leveled out the rejection coefficient effect into a linear reduction as the permeability of each pass/stage was set independently. Overall, this showed that a continuous ILDF process would minimize any impact of the EtOH rejection coefficient or permeability reduction as compared to the batch CVDF process.

3.2.4 | Continuous ILDF buffer consumption

Another means of evaluating the continuous ILDF process versus the batch process involves comparing buffer consumption. Buffer consumption, in this case, included the buffer needed for the initial dilution of the starting liposome formation mixture as well as that needed to perform the diafiltration to the target EtOH concentration. Figure 5 shows the buffer consumption (dilution and diafiltration) for theoretical batch processes of equivalent scale with rejection coefficients of 0 and 0.5 (the approximate value of previously calculated batch scenario) and compares them to the continuous ILDF model used to generate the results in Figures 4B. Surprisingly, the continuous ILDF set up is in line with the zero rejection coefficient batch process. Previous evaluations of similar set ups in the realm of biologics have shown continuous designs to require more buffer than batch.[24,25] The Figure 5 results again show how the use of independent passes/stages offsets the impact of EtOH on the hollow fiber permeability.

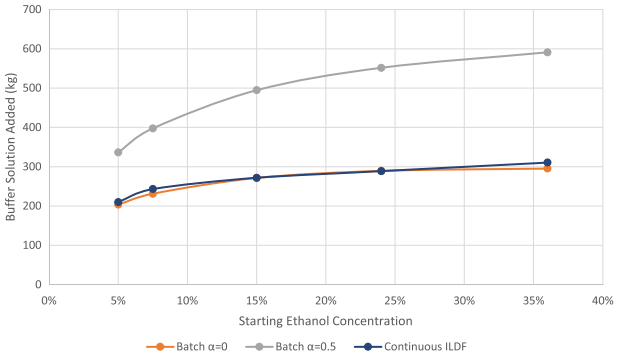

FIGURE 5 Buffer required (Dilution + Diafiltration) to achieve target ethanol removal when using various initial ethanol concentration for theoretical batch processes with rejection coefficient of 0 and 0.5 and a continuous inline-diafiltration (ILDF) process as calculated in Figure 4B.

4 | DISCUSSION

The assessment of the continuous ILDF set up for liposomal drug product formulation refinement was successful and provided a range of intriguing results. The notion of the permeate being impacted by the EtOH concentration in the batch process was reinforced by the results from the continuous ILDF experiment(s).

The use of the simulated ILDF (Figure 1D) showed that reduction of the initial EtOH concentration produced an EtOH concentration dependent rate of reduction in the number of passes/stages necessary to achieve the target EtOH removal. This led to the derivation of an equation (Equation 2) for the simulated ILDF concentration/dilution arrangement (Figure 1D) including the derivation of a function for EtOH concentration dependency of the rejection coefficient (Equation 3).

While these equations prove applicable and predictable under the simulated ILDF set up from Figure 1D, these equations proved less applicable to a real-world set up such as that shown in Figure 1C. The simulated ILDF method showed that the permeability of the hollow fiber was limited by the initial exposure of EtOH. The permeability then only improved a limited amount as the EtOH concentration decreased with each pass. By using the same hollow fiber to simulate each pass of a ILDF system, the efficiency of each subsequent pass was limited

and not representative of a true ILDF arrangement. By using the data from the initial passes of the separate runs, a true ILDF data set was extrapolated and assessed.

The continuous ILDF model showed an almost linear reduction as compared to the exponential reduction in the simulated ILDF model (Figure 4B vs. Figure 3B). This may be because the permeability of the hollow fibers in the continuous ILDF model were set independently and had no impact on the subsequent hollow fibers as the EtOH concentration decreased. Additionally, the linear reduction of the EtOH in the continuous ILDF model limited the overall buffer consumption to that of a batch process where the rejection coefficient is zero. This showed that continuous ILDF would be more efficient than a solvent-based batch TFF with respect to buffer required.

Based on these findings, the impact of EtOH on the continuous ILDF design is less driven by a traditional rejection coefficient concept and more on EtOH's effect on hollow fiber permeability. By reducing the initial exposure of each individual hollow fiber in a continuous ILDF system, the performance and overall efficiency of the system is improved. The most optimal design for a liposomal continuous ILDF process would involve significant upfront dilution (i.e., 5% initial EtOH concentration) in order to start the ILDF with minimal EtOH concentration. This would minimize the amount of ILDF stages needed and buffer required. This is similar to the dilution strategy recommended for albumin diafiltration though optimization is not specifically correlated to the impact of EtOH concentration on permeability.[26,27] Additionally, these finding may prove applicable and beneficial to mRNA-LNP vaccines, which often look to minimize mRNA exposure to organic solvents as well as having massive production demands,[28–30] which a continuous process design could help to meet.

5 | CONCLUSIONS

Continuous manufacturing designs for liposomal drug products will help meet the demand for these formulations, which are critical for future drug delivery options. Understanding what impacts these continuous manufacturing designs has benefit to their optimization. What is viewed to be a minor phenomenon in a batch process design could have significant impact to a continuous design. The deduction of an EtOH concentration-dependent rejection coefficient in the batch process has led to a greater understanding of how EtOH concentration will impact a continuous TFF/ILDF process. EtOH reduces and limits hollow fiber permeability with the impact increasing with concentration. It was determined that by diluting the post-liposome formation bulk and reducing the initial EtOH concentration that fewer passes/stages of ILDF and less buffer would be needed to achieve target EtOH removal. In understanding this impact, continuous ILDF presents as a competitive alternative to the batch process that can be scaled at will.

AUTHOR CONTRIBUTIONS

Vaughan Thomas: Formal analysis, investigation, writing – review & editing. Suzanne S. Farid: Formal analysis, investigation, writing – review & editing.

ACKNOWLEDGMENTS

UCL Biochemical Engineering hosts the Future Targeted Healthcare Manufacturing Hub in collaboration with UK universities and with funding from the UK Engineering & Physical Sciences Research Council (EPSRC) and a consortium of industrial users and sector organizations (Grant Ref: EP/P006485/1).

CONFLICT OF INTEREST STATEMENT

The authors declare no financial or commercial conflict of interest.

DATA AVAILABILITY STATEMENT

The data that support the findings of this study are available from the corresponding author upon reasonable request.

ORCID

Robert D. Worsham https://orcid.org/0009-0002-5346-7651

REFERENCES

1. Akbarzadeh, A., Rezaei-Sadabady, R., Davaran, S., Joo, S. W., Zarghami, N., Hanifehpour, Y., Samiei, M., Kouhi, M., & Nejati-Koshki, K. (2013). Liposome: Classification, preparation, and applications. *Nanoscale Research Letters*, *8*, 102.
2. Maherani, B., Arab-Tehrany, E., Mozafari, M. R., Gaiani, C., & Linder, M. (2011). Liposomes: A review of manufacturing techniques and targeting strategies. *Current Nanoscience*, *7*(3), 436–445.
3. Mozafari, M. R. (2005). Liposomes: An overview of manufacturing techniques. *Cellular & Molecular Biology Letters*, *10*(4), 711–719.
4. Worsham, R., Thomas, V., & Farid, S. (2018). Potential of continuous manufacturing for liposomal drug products. *Biotechnology Journal*, *14*(2), e1700740.
5. Jaafar-Maalej, C., Diab, R., Andrieu, V., Elaissari, A., & Fessi, H. (2010). Ethanol injection method for hydrophilic and lipophilic drug-loaded liposome preparation. *Journal of Liposome Research*, *20*(3), 228–243.
6. Wagner, A., & Vorauer-Uhl, K. (2011). Liposome technology for industrial purposes. *Journal of Drug Delivery*, *2011*, 591325. https://doi.org/10.1155/2011/591325
7. Wagner, A., Vorauer-Uhl, K., Kreismayr, G., & Katinger, H. (2002). The crossflow injection technique: An improvement of the ethanol injection method. *Journal of Liposome Research*, *12*(3), 259–270.
8. Wagner, A., Vorauer-Uhl, K., Kreismayr, G., & Katinger, H. (2002). Enhanced protein loading into liposomes by the multiple crossflow injection technique. *Journal of Liposome Research*, *12*(3), 271–283.
9. Wagner, A., Vorauer-Uhlb, K., & Katinger, H. (2002). Liposomes produced in a pilot scale: Production, purification and efficiency aspects. *European Journal of Pharmaceutics and Biopharmaceutics*, *54*, 213–219.
10. Kim, S., Kim, T., & Murdande, S. (2012). *Sustained-release liposomal anesthetic compositions* (US Patent, 8. 182,835 B2).
11. Li, Z., Boni, L., Miller, B., Malinin, V., & Li, X. (2011). *High delivery rates for lipid based drug formulations and methods of treatment thereof* (US Patent, 7. 879,351 B2).
12. Castilho, L. (2015). Continuous animal cell perfusion processes: The first step toward integrated continuous manufacturing. In Subramanian, G. (Ed.), *Continuous process in pharmaceutical manufacturing* (pp. 115–153). Wiley-VCH.
13. Pollock, J., Bolton, G., Coffman, J., Ho, S., Bracewell, D., & Farid, S. (2023). Optimising the design and operation of semi-continuous affinity chromatography for clinical and commercial manufacture. *Journal of Chromatography A*, *5*(1284), 17–27.
14. Whitford, W. (2015). Single-use systems support continuous bioprocessing by perfusion culture. In Subramanian, G. (Ed.), *Continuous process in pharmaceutical manufacturing* (pp. 183–226). Wiley-VCH.

15. Arunkumar, A., Singh, N., Peck, M., & Li, Z. (2017). Investigation of single-pass tangential flow filtration (SPTFF) as an inline concentration step for cell culture harvest. *Journal of Membrane Science*, *524*, 20–32.
16. Brower, M., Hou, Y., & Pollard, D. (2015). Monoclonal antibody continuous processing enabled by single use. In Subramanian, G. (Ed.), *Continuous process in pharmaceutical manufacturing* (pp. 255–296). Wiley-VCH.
17. Casey, C., Gallos, T., Ayturk, E., & Pearl, S. (2011). Protein concentration with single-pass tangential flow filtration (SPTFF). *Journal of Membrane Science*, *384*, 82–88.
18. Dizon-Maspat, J., Bourret, J., D'Agostini, A., & Li, F. (2012). Single pass tangential flow filtration to debottleneck downstream processing for therapeutic antibody production. *Biotechnology and Bioengineering*, *4*, 962–970.
19. Jungbauer, A. (2013). Continuous downstream processing of biopharmaceuticals. *Trends in Biotechnology*, *31*(8), 479–492.
20. Subramanian, G. (Ed.). (2015). *Continuous process in pharmaceutical manufacturing*. Wiley-VCH.
21. Gjoka, X., Gantier, R., & Schofield, M. (2017). Platform for integrated continuous bioprocessing. *BioPharm International*, *30*(7), 26–32.
22. Kochan, J., Wintgens, T., Hochstrat, R., & Melin, T. (2009). Impact of wetting agents on the filtration performance of polymeric ultrafiltration membranes. *Desalination*, *241*, 34–42.
23. Otitoju, T. A., Ahmad, A. L., & Ooi, B. S. (2017). Influence of ethanol as bore fluid component on the morphological structure and performance of PES hollow fiber membrane for oil in water separation. *Korean Journal of Chemical Engineering*, *34*(10), 2703–2709.
24. Jabra, M., Yehl, C., & Zydney, A. (2019). Multistage continuous countercurrent diafiltration for formulation of monoclonal antibodies. *Biotechnology Progress*, *35*(4), e2810.
25. Kavara, A., Sokolowski, D., Collins, M., & Schofield, M. (2020). Chapter 4 – Recent advances in continuous downstream processing of antibodies and related products. In *Characterization of antibody-based therapeutics* (pp. 81–103). Elsevier.
26. Jaffrin, M. Y., & Charrier, J. P. (1994). Optimization of ultrafiltration and diafiltration processes for albumin production. *Journal of Membrane Science*, *97*, 71–81.
27. Paulen, R., Fikar, M., Kovacs, Z., & Czermak, P. (2011). Process optimization of diafiltration with time-dependent water adding of albumin production. *Chemical Engineering and Processing: Process Intensification*, *50*, 815–821.
28. Hou, X., Zaks, T., Langer, R., & Dong, Y. (2021). Lipid nanoparticles for mRNA delivery. *Nature Review Materials*, *6*, 1078–1094.
29. Schoenmaker, L., Witzigmann, D., Kulkarni, J., Verbeke, R., Kersten, G., Jiskoot, W., & Crommelin, D. (2021). mRNA-lipid nanoparticle COVID-19 vaccines: Structure and stability. *International Journal of Pharmaceutics*, *601*, 120586.
30. Verma, M., Ozer, I., Xie, W., Gallagher, R., Teixeira, A., & Choy, M. (2023). The landscape for lipid-nanoparticle-based genomic medicines. *Nature Reviews Drug Discovery*, *22*(5), 349–350. https://doi.org/10.1038/d41573-023-00002-2

How to cite this article: Worsham, R. D., Thomas, V., & Farid, S. S. (2023). Impact of ethanol on continuous inline diafiltration of liposomal drug products. *Biotechnology Journal*, e2300194. https://doi.org/10.1002/biot.202300194